J. Am. Soc. Mass Spectrom (2011) 22:817–827
DOI: 10.1007/s13361-011-0105-0

RESEARCH ARTICLE

Complexation of Amino Compounds by 18C6 Improves Selectivity by IMS-IMS-MS: Application to Petroleum Characterization

Zhiyu Li, Stephen J. Valentine, David E. Clemmer

Department of Chemistry, Indiana University, 800 E. Kirkwood Ave., Bloomington, IN, 47405, USA

Abstract

Complexation of a series of related amino compounds by 18-crown-6 ether (18C6) is studied as a means of improving the resolution of mixtures by combinations of ion mobility spectrometry (IMS) and mass spectrometry (MS) techniques. Mixtures of the isomeric amines n-octylamine (NOA), dibutylamine (DBA), and diisopropylethylamine (DIPEA) were electrosprayed to produce gaseous $[M + H]^+$ ions. These species have overlapping mobilities and are not resolved by IMS. Addition of 18C6 yields $[M + 18C6 + H]^+$ ion complexes that are resolved by IMS. In subsequent experiments, $[M + 18C6 + H]^+$ ion complexes are separated according to their mobilities and specific species are selected and exposed to collisional activation. This analysis yields dissociation voltages that are inversely correlated with the number of separate substitutions on the nitrogen atom of the amino compounds; dissociation voltages of ~40, ~90, and ~150 V are obtained for the tri-, di-, and mono-substituted amino compounds DIPEA, DBA, and NOA, respectively. For these complexes, an inverse correlation is also observed with respect to the gas-phase basicities (GB) of the amino compounds (964, 935, and 895 kJ mol^{-1}, respectively). Studies of 18C6 complexes with a series of n-alkylamines ($C_nH_{2n+3}N$ where n=3 to 18, respectively) show that dissociation voltages increase systematically (from ~140 to ~190 V) under the conditions employed. The sensitivity to collision energy provides an additional means of distinguishing between classes of compounds. The approach is extended as a means of separating nitrogen-containing compounds from petroleum.

Key words: Petroleomics, Ion mobility spectrometry, Separation selectivity, Crown Ether Complexation

Introduction

Ion mobility spectrometry (IMS) is an analytical technique that separates gas-phase ions based on differences in their mobilities through an inert buffer gas under the influence of a uniform electric field [1]. The technique is used for the detection of a variety of molecular compounds including drugs, explosives, and chemical warfare agents [2–8]. Recently, nested IMS-mass spectrometry (MS) instrumentation has been developed as a high-speed method for analysis of extremely complex mixtures [9–18]. In addition to the speed of analysis, IMS-MS analysis makes it possible to distinguish ions of the same mass-to-charge ratio (m/z) [19–27], and thus has potential as a means of characterizing mixtures of isomers.

A limitation of these analyses arises from the intrinsic correlation of ions' physical sizes with their masses. This correlation ultimately limits the peak capacity of the two-dimensional IMS-MS approach. Analysis of large peptide mixtures shows that for IMS instruments with resolving powers of 20 to 100, an ~3- to ~10-fold increase in peak capacity is obtained with the IMS-MS combination compared with MS alone [12, 28]. Because of its potential for complex mixture characterization, significant work has focused on improving IMS resolution capabilities; several high-resolution instruments are capable of resolving powers [defined as $R = \frac{t}{\Delta t}$, where t is the drift time of the ion and Δt

Correspondence to: David E. Clemmer; *e-mail:* Clemmer@indiana.edu

Received: 24 November 2010
Revised: 2 February 2011
Accepted: 9 February 2011
Published online: 24 March 2011

is the full width at half maximum (FWHM) of the peak] in the range of ~100 to ~200 [12, 29–36]. Higher resolution IMS measurements are possible [37–40] but are still at an early stage of development.

Recently, several studies have focused on improving the efficiency of IMS measurements by using two-dimensional mobility separations [33, 34, 41–47]. In the IMS-IMS strategy pursued in our laboratory, ion structures (which influence the ions' mobilities) are altered between the two separation steps. Substantial increase in the peak capacity is observed; capacities of ~500 to ~1500 were estimated for IMS-IMS measurements of peptide ions [42]. By multiplexing the mobility selection process, such separation efficiency can be gained without significantly increasing analysis times [44–47]. Other approaches for improving experimental sensitivity for IMS analyses include ion focusing techniques and multiplexing strategies [32, 35, 48–50].

Changing the ions' structures offers a simple means of influencing the size/mass correlation; another approach is to change the ions' masses in addition to their physical size. Several groups have explored the use of selective complexation reagents for improving separations. Cyclic polyether (crown ether) and acyclic polyether shift reagents were used in IMS-MS analyses of amines [26, 51, 52], amino acids [53], peptides [53, 54], and active pharmaceutical components [55]. These reagents are interesting because a substantial understanding of the interactions of these molecules exists. For example, the gas-phase stabilities of polyether complexes with ammonium [56, 57], metal ions [58, 59], amines [51, 52, 57, 60], and peptides [61] were studied. For amines and peptides, ion complex stabilities depend on the types of polyethers used, the gas-phase basicity (GB) of the ion, and the structures of the amines and peptides. Subtle structural changes in the amines and peptides result in measurable changes in the stabilities of the ion complexes [51, 60, 61].

The studies presented below describe the combination of multidimensional IMS separations [33, 34, 42–47] with the use of non-covalent, 18C6–ion complexes for improved resolution of amino compounds in mixtures. For a mixture of three molecular isomers, the addition of 18C6 allows the resolution of two isomer ions with overlapping mobilities for $[M + H]^+$ ions. The use of an energy-variable dissociation step performed between the mobility separations is used to further isolate amino compounds. In general, the relative stabilities of 18C6–ion complexes are observed to inversely correlate with values of GB for the amino compounds. Additional experiments show that, for a series of n-alkylamines, ion complex stabilities increase with increasing molecular size.

The utility of 18C6 complexation and IMS-IMS techniques is demonstrated as a means of obtaining increased resolution of mixture components for a vacuum gas oil (VGO) distillate sample. Previous efforts have applied IMS-MS techniques to the characterization of petroleomics samples and have demonstrated a ~3- to ~5-fold improvement in component resolution compared with MS alone [62, 63]. In influencing the size/mass correlation of ions, 18C6 ion complexation can extend the utility of IMS-MS analyses by allowing characterizations of select molecular subgroups obtained from complex mixtures. Because the technique results in mass shifts of select ions, such analyses may also find practice for enhancing high-resolution MS characterizations of complex petroleomics mixtures [64–69].

Experimental

Overview of the IMS-IMS-MS Instrument

Detailed descriptions of IMS-MS theory [1, 11, 17, 70] and instrumentation [9, 13, 33, 34, 42, 54, 71–74] have been provided elsewhere, and only a brief description of the instrument used in these studies as well as operational modes is presented here. The work presented here is influenced by studies conducted nearly a decade ago with the first demonstration of the parallel dissociation of a distribution of mobility-dispersed precursor ions [72]. This approach was later utilized in experiments demonstrating crown ether complexation with peptide ions as a means to improve mobility separation efficiency [54]. Figure 1 shows a schematic of the IMS-IMS-MS instrument used for these studies. The instrument consists of a standard electrospray source equipped with a Smith geometry ion funnel (F1) [75–77] mounted to the front of a drift tube/time-of-flight (TOF) instrument. The drift tube assembly is comprised of two drift regions (D1 and D2) connected in series by an ion funnel (F2). The instrument used for this study can be operated in different modes, such as ion selection, ion activation, and ion fragmentation by changing the voltage settings at the G2 and IA2 regions (Figure 1) of the drift tube as described previously [33, 34, 42–44].

Ions generated by electrospray ionization (ESI) are introduced directly into the first ion funnel (F1), where they are accumulated. Concentrated ion packets are then periodically gated into the first drift region (D1) via an electrostatic gate (G1). The ions migrate through D1 under the influence of a uniform electric field (~10 $V cm^{-1}$) and collide with the He buffer gas (ultra high purity; Airgas, Radnor, PA, USA) maintained at a pressure of ~3 Torr and a temperature of ~300 K. The electric field and buffer gas pressure conditions are maintained such that IMS measurements are carried out in the low field region ($E/p<20$ to 45 $V cm^{-1}$ $Torr^{-1}$ for ions with m/z of 500 to 2500) [1, 4]. As ions exit D1, they enter the second ion funnel region (G2/F2/IA2). At the entrance of the second ion funnel (F2) there is a second electrostatic gate (G2) that can either be set to transmit or select specific components of the ion mixture. Subsequently, in F2, the diffuse ion cloud is focused toward the center of the drift tube, and can be energized by increasing the voltage (5 to 200 V) between the last two lenses (spaced apart by 3.2 mm) of this region (IA2, Figure 1). A value of 20 V across the two adjacent lenses

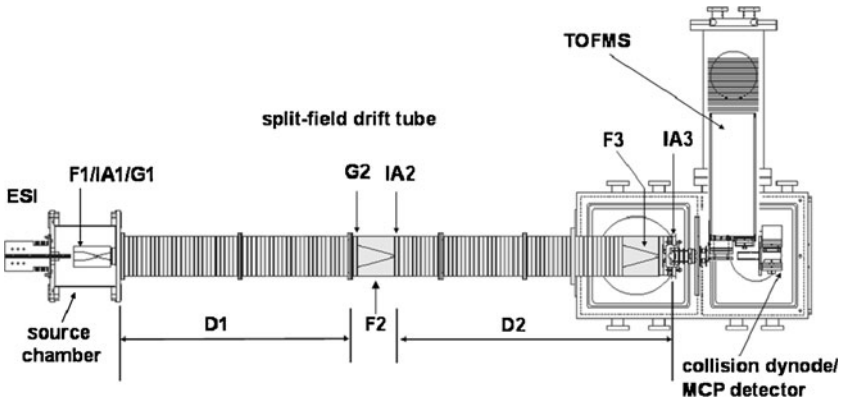

Figure 1. Schematic diagram of the IMS/IMS/MS instrument used in these experiments. See text for details of instrument operation

comprising IA2 (6.3×10^3 V m^{-1}) is considered to be the threshold for ion activation. The ions transmitted into the second drift region (D2) also migrate through this device under the influence of an electric field and collide with He buffer gas atoms under the same operating conditions as those used for the D1 region. After exiting D2, the ions are again focused in the third ion funnel (F3) before exiting the high-pressure region. Upon introduction into the high-vacuum region, ions are focused into the source of a TOF mass spectrometer and their masses are analyzed. As described previously, ion flight times in the mass spectrometer are much shorter than drift times, making it possible to record data in a nested fashion [9].

The total length of the IMS-IMS drift tube is ~183 cm. Separately, D1 is 71.3 cm, D2 is 98.5 cm, and F2 is 13.0 cm. The drift regions D1 and D2 are operated at ~10 Vcm^{-1}, the fields through the ion funnels are ~11 Vcm^{-1}, and the RF voltages in the funnels are ~130 $V_{p\text{-}p}$ at frequencies of 390 to 460 kHz. The buffer gas is maintained at 300 K.

Materials

18-Crown-6 (18C6, 99%) and all amino compounds (>98%) were purchased from the Sigma-Aldrich Co. (St. Louis, MO, USA) and used without further purification. Water, methanol, toluene, and acetic acid (HPLC grade) were purchased from EMD Chemicals (Gibbstown, NJ, USA). A low-boiling point fraction of VGO distillate (~295 to 319 °C) was provided as a gift courtesy of ExxonMobil (ExxonMobil Research and Engineering Company, Annandale, NJ, USA).

ESI Conditions

The amino compound samples and the VGO sample are electrosprayed from a methanol:toluene (50:50) solution with 1% acetic acid by volume. The concentration of the pure amino compounds is typically ~0.01 mg ml^{-1} and the concentration of the VGO distillate sample is ~2.0 mg ml^{-1}. The concentration of 18C6 in each mixture is typically 5 to 10 times the concentration of the other analyte by mass. All samples are infused at a flow rate of ~0.30 μL min^{-1} by a syringe pump (KD Scientific, Holliston, MA, USA) and are electrosprayed with a pulled-tip capillary (75 µm i.d.× 360 µm o.d., Polymicro Technologies, Phoenix, AZ, USA) that is maintained at a voltage of ~2.2 kV relative to the source entrance plate.

Data Evaluation

The Origin 8 software suite (OriginLab Corp., Northampton, MA, USA) has been used to create two-dimensional dot plots depicting ion intensities as a function of drift time and m/z value [$t_D(m/z)$ distribution]. It has also been employed to fit the features in the datasets. Algorithms developed in house have been used for extracting portions of the two-dimensional data for specific analyses. The m/z values of $[M + H]^+$ ions are obtained from a multipoint calibration.

Results and Discussion

18C6 as a Shift Reagent for Model Amino Compounds

The isomeric amines n-octylamine (NOA), dibutylamine (DBA), and diisopropylethylamine (DIPEA) have the same elemental composition ($C_8H_{19}N$) and, thus, the $[M + H]^+$ ion of each compound has the same monoisotopic m/z of 130.160. The property of identical mass makes it impossible to distinguish the three amines by high-resolution mass spectrometry alone. Figure 2 shows the nested two-dimensional, $t_D(m/z)$ plots of datasets obtained from the pure amino compound mixture and the mixture with 18C6. Dataset feature assignments were obtained from individual analyses (not shown here). In each individual sample (without 18C6), $[M + H]^+$ ions are primarily formed. For IMS-MS analyses of the amino compound mixture (Figure 2a), all ions are transmitted through G2 into the D2 region. With this single mobility separation step, $[DIPEA + H]^+$ ions (t_D~9.0 ms) are baseline resolved from $[DBA + H]^+$ ions (t_D~9.8 ms) and $[NOA + H]^+$ ions (t_D~9.9 ms). However, $[DBA + H]^+$ and $[NOA + H]^+$ ions show a significant level of overlap in drift time.

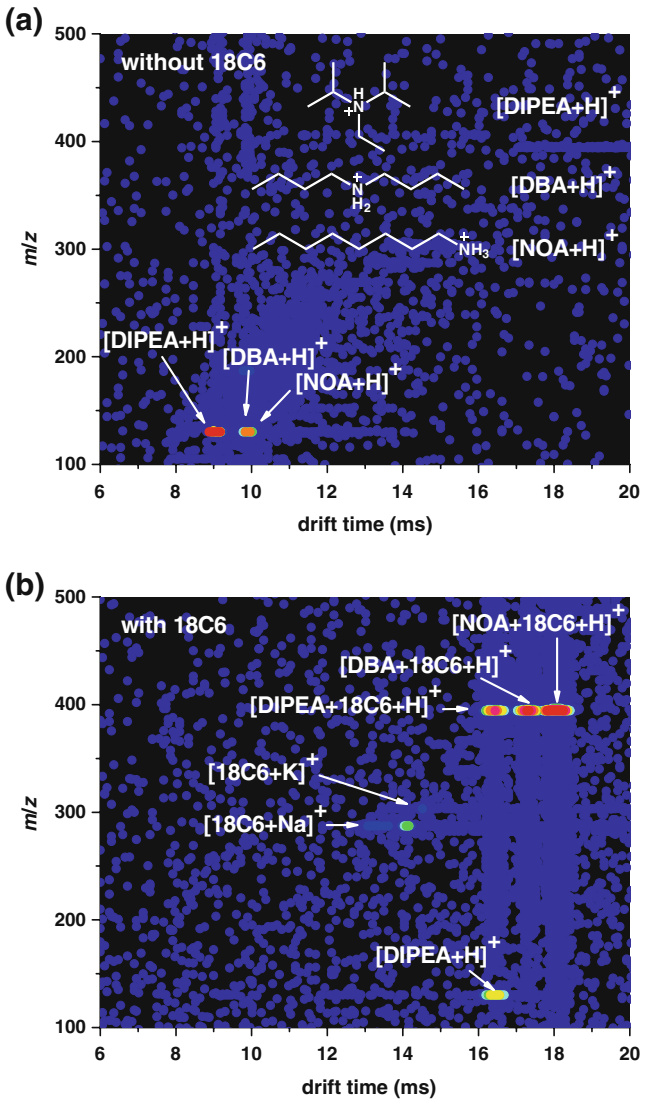

Figure 2. Two-dimensional dot plots of drift time versus *m/z* obtained from ESI-IMS-MS experiments for amino compound mixtures. Panel (**a**) shows data for a mixture of 1:1:1 DIPEA, DBA, and NOA. Panel (**b**) shows data for a mixture of 1:1:1 DIPEA, DBA, and NOA with the incorporation of 18C6 in each sample. The $[M + H]^+$ and $[M + 18C6 + H]^+$ ions are identified by individual analyses (not shown here). The intensities of different features are represented here using a false color scheme in which the least intense features are shown in dark blue and the most intense are shown in red. The structures of the $[M + H]^+$ ions are shown as an inset in Figure 2a

When 18C6 is added to the sample solutions (containing only a single analyte), $[M + 18C6 + H]^+$ ions are primarily formed. Also, under these conditions, ions related to 18C6, such as $[18C6 + H]^+$ (m/z=265.165), $[18C6 + Na]^+$ (m/z=287.147) and $[18C6 + K]^+$ (m/z=303.121) are also observed. These crown ether ions exhibit relatively high ion intensities so that in order to focus on $[M + 18C6 + H]^+$ ion complexes, only the drift time region corresponding to these ions has been selected at G2 to be transmitted into the D2 region (see Experimental section). Figure 2b shows that the three ion complexes, $[DIPEA + 18C6 + H]^+$ (t_D~16.4 ms), $[DBA + 18C6 + H]^+$ (t_D~17.3 ms), and $[NOA + 18C6 + H]^+$ (t_D~18.1 ms) are baseline resolved. A small amount of $[DIPEA + 18C6 + H]^+$ ions that dissociate into $[DIPEA + H]^+$ ions at the end of the drift tube prior to TOF analysis is also observed. A comparison of Figure 2a and b suggests that the use of 18C6 for complexation with small amino compounds can help to resolve some molecules with very similar mobilities.

18C6 As an Energy-Dependent Shift Reagent

It is instructive to consider structural aspects of various molecules in a mixture in order to consider applications of specific shift reagents. For amines and peptides, it is known that the stabilities of $[M + 18C6 + H]^+$ ion complexes can be affected by subtle structural differences in the small molecules [51, 60, 61]. Such a characteristic of 18C6–ion complexes may provide a mechanism for an additional dimension of separation resulting in an increased peak capacity for the IMS-IMS-MS method.

Figure 3 shows nested two-dimensional, $t_D(m/z)$ plots obtained upon activation of the $[C_8H_{19}N + 18C6 + H]^+$ mixture using different activation energies (Figure 3a: 70 V, and Figure 3b: 100 V) in the IA2 region (Figure 1). Upon activation at 70 V, most $[DIPEA + 18C6 + H]^+$ ions dissociate to form $[DIPEA + H]^+$ (Figure 3a), while most $[DBA + 18C6 + H]^+$ and $[NOA + 18C6 + H]^+$ ions remain intact. Because the dissociation occurs after D1 (Figure 1), the two remaining complexes and the $[DIPEA + H]^+$ ions have significantly different drift times (~6 ms) as well as m/z values. When an activation voltage of 100 V is applied (Figure 3b), the majority of the $[DIPEA + 18C6 + H]^+$ ions and the $[DBA + 18C6 + H]^+$ ions dissociates into $[DIPEA + H]^+$ and $[DBA + H]^+$ ions, respectively. Only the $[NOA + 18C6 + H]^+$ ion complex remains intact.

The dissociation selectivity of 18C6-ion complexes in IMS-IMS instrumentation can be investigated using a number of different sample compounds. Figure 4 shows the dissociation percentage as a function of activation voltage for several 18C6–ion complexes as well as 18C6-n-alkylamine ion complexes obtained from similar IMS-IMS-MS experiments. Figure 4a shows the data for ion complexes of the amino compound isomers each having the same nominal mass (129 Da) but different nitrogen structures [i.e., primary (1°), secondary (2°), or tertiary (3°) amines]. $[DIPEA + 18C6 + H]^+$ ion complexes (3° amine) have a relatively low gas-phase stability (dissociating between ~20 V and ~60 V); $[DBA + 18C6 + H]^+$ ion complexes (2° amine) have higher gas-phase stabilities (dissociating between ~60 V and ~100 V); and, 18C6 complexes of NOA (Figure 4a) as well as other n-alkylamines with 1° amines (Figure 4b) have the highest gas phase stabilities (dissociation voltages >100 V). Interestingly

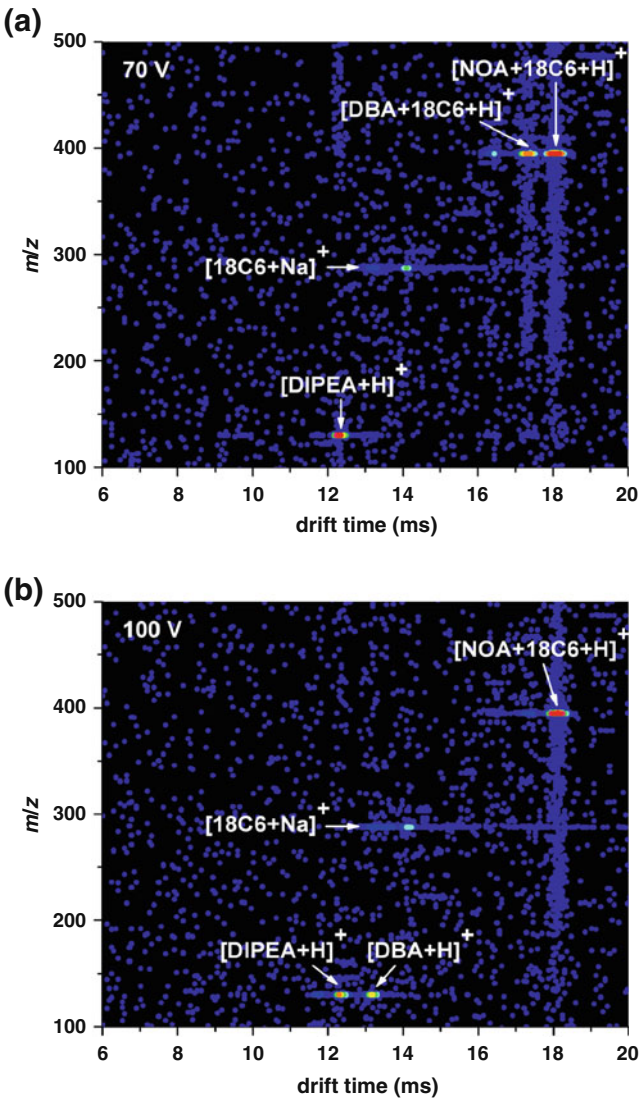

Figure 3. Two dimensional dot plots of drift time versus *m/z* obtained from ESI-IMS-MS experiments for a mixture of 1:1:1 DIPEA, DBA and NOA with the incorporation of 18C6 in each sample under different activation voltages applied at IA2. Panel (**a**) shows data collected using an activation voltage of 70 V. Panel (**b**) shows data collected using 100 V. The $[M + H]^+$ and $[M + 18C6 + H]^+$ ions are identified by individual analyses (not shown here). The intensities of different features are represented here using a false color scheme in which the least intense features are shown in dark blue and the most intense are shown in red

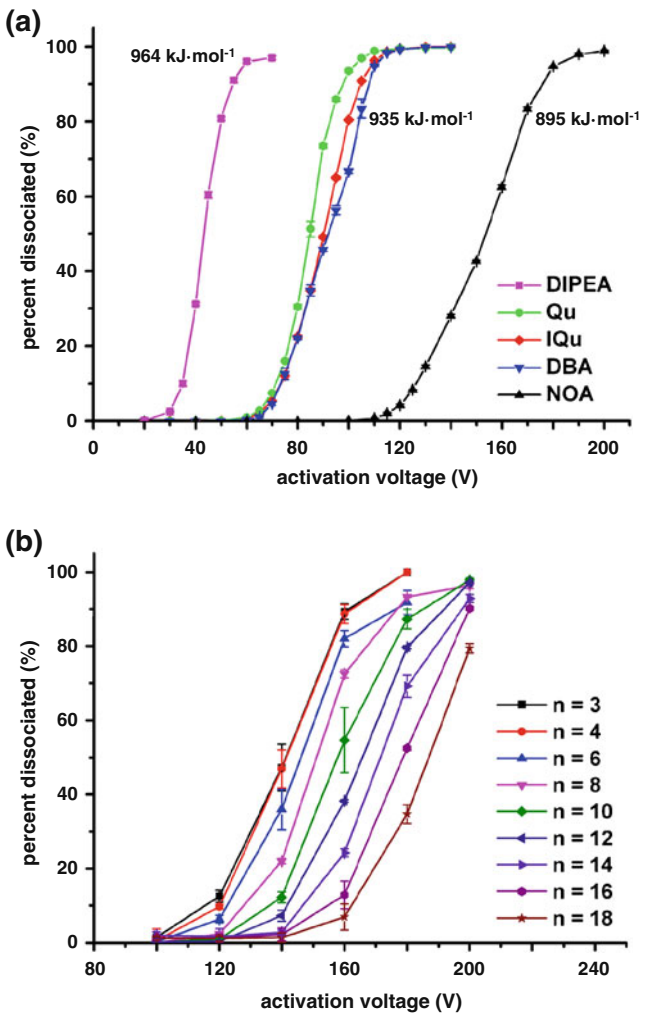

Figure 4. Plots of dissociation percentages for a series of 18C6-ion complexes. Panel (**a**) shows dissociation percentages for complexes formed from isomeric amino compounds (NOA, DBA, and DIPEA) as well as the isobaric compounds Qu and IQu each with the same nominal mass of 129. GB values are listed for DIPEA, DBA, and NOA. All ion abbreviations are associated with molecules in the text. Panel (**b**) shows dissociation percentages for complexes formed by n-alkylamines of different lengths each containing a 1° amine group. Ion assignments in terms of the number of carbons in the molecule ($C_nH_{2n+3}N$) are provided as a key

18C6 complexes of quinoline (Qu) and isoquinoline (IQu) [3° amines with the same nominal mass (129) as the three isomers] have gas-phase stabilities that are similar to the $[DBA + 18C6 + H]^+$ ion complexes. Figure 4b illustrates the voltage-dependent dissociation of [n-alkylamine + 18C6 + $H]^+$ ion complexes which have identical amine structures but different molecular masses. The data show that dissociation voltage increases with increasing ion size for these 1° amines.

Predicting Dissociation Voltage Based on Amino Compound Properties

The utility of 18C6 ion complexation with IMS-IMS-MS characterization may find significant utility as a means of simplifying complex mixtures in order to enhance the resolution of specific components. Therefore, an understanding of factors affecting the stabilities of 18C6–ion complexes will affect the ability to use the method for complex mixture characterization. Table 1 lists the amino compounds tested in this study along with ion complex dissociation voltages (obtained from the 50% dissociation values in Figure 4) and gas-phase thermochemical information.

Table 1. IMS-IMS dissociation voltage values for the $[M + 18C6 + H]^+$ complexes of the various amino compounds

Molecule	Molecular formula	Mass (Da)[a]	Dissociation voltage (V)[b]	Gas-phase basicity ($kJ \cdot mol^{-1}$)[c]
n-Propylamine	C_3H_9N	59.073	141	884
n-Butylamine	$C_4H_{11}N$	73.089	141	887
n-Hexylamine	$C_6H_{15}N$	101.120	146	894
n-Octylamine	$C_8H_{19}N$	129.152	151	895
Dibutylamine	$C_8H_{19}N$	129.152	92	935
Diisopropylethylamine	$C_8H_{19}N$	129.152	43	964
Quinoline	C_9H_7N	129.058	85	921
Isoquinoline	C_9H_7N	129.058	90	920
n-Decylamine	$C_{10}H_{23}N$	157.183	158	897
n-Dodecylamine	$C_{12}H_{27}N$	185.214	166	NA
n-Tetradecylamine	$C_{14}H_{31}N$	213.246	171	NA
n-Hexyldecylamine	$C_{16}H_{35}N$	241.277	179	NA
n-Octyldecylamine	$C_{18}H_{39}N$	269.308	187	NA

[a]Monoisotopic masses have been calculated according to the molecular formulae
[b]Dissociation voltages are defined at 50% ion complex abundance as shown in Figure 4
[c]Gas phase basicities are obtained from reference 79

Table 1 and Figure 4 show that, in general, dissociation voltages increase with a decrease in the number of substitutions at the nitrogen atom. For example, the ordering of dissociation voltages for the model isomeric amines is DIPEA (43 V) << DBA (92 V) << NOA (151 V). Here we note that the number of separate substitutions on the nitrogen atoms is three, two, and one, for the respective compounds, and that the relative ordering of dissociation voltages is likely to result in large part from the number of available hydrogen bonds with the amine; for ammonium/polyether complexes, additional hydrogen bonds (compared with a single interaction) may provide up to 88 kJ mol^{-1} of additional binding energy [57, 78]. For the respective compounds, an inverse correlation between dissociation voltage and GB of the amino compound is also observed ($GB_{DIPEA} \approx 964$ kJ mol^{-1}, $GB_{DBA} \approx 935$ kJ mol^{-1}, and $GB_{NOA} \approx 895$ kJ mol^{-1}) [79].

Dissociation voltages for Qu (85 V) and IQu (90 V) are similar to that observed for DBA (92 V). This comparison is instructive because Qu and IQu are compounds containing 3° amines while DBA contains a 2° amine. Thus, the similarity in complex stability for these three compounds cannot solely be ascribed to the number of available hydrogen bonds. It is noteworthy that these three compounds share the characteristic of having only two separate carbons bonded to the nitrogen atoms. For these 3° amines it appears that decreased steric effects increase the overall stability of the complex; that is, there is greater accessibility to the charge site for these compounds when compared to the 3° amine DIPEA. It is noted that GB values for Qu and IQu are 921 and 920 kJ mol^{-1}, respectively, and are more similar to that of DBA.

For the n-alkylamine complexes (Figure 4b), the dissociation voltages do not inversely correlate with GB. As an example, consider octylamine ($GB \approx 895$ kJ mol^{-1}) and propylamine ($GB \approx 884$ kJ mol^{-1}). 18C6 complexes with these molecules have dissociation voltages of ~152 and ~142 V, respectively. The observed relative stabilities of the n-alkylamines may be reflective of the overall complex size and the collision dynamics in the ion activation region. For example, under the conditions employed in the present experiments, the number of collisions experienced in the IA2 region of the instrument for these alkylamines ranges from ~50 to ~300. For larger complexes, the energy imparted into the ion complex with each collision is dispersed among a greater number of internal modes, thereby requiring higher voltage settings to be used in order to induce dissociation. This also may explain the fact that the dissociation curves of the larger complexes have larger variances than those of the smaller complexes.

The results shown in Figure 4 suggest that the stabilities of such compounds are governed by several factors. These include the number of separate substitutions on the nitrogen atom of the compound, steric factors affecting charge site accessibility, as well as the overall size of the amine compound. The wide range of differences in dissociation voltage thresholds associated with these factors suggests that it may be possible to provide a gross estimation of complex dissociation voltages for a variety of amino compounds. Additionally, the large range in dissociation voltages suggests the possibility of using voltage settings to isolate specific compounds with reasonable selectivity. Figures 3 and 4 demonstrate the separation potential of the use of 18C6 as an energy-dependent shift reagent in IMS-IMS measurements, and it is worthwhile to consider the approach for resolving nitrogen-containing compounds in complex mixtures such as those encountered in petroleomic characterizations. It is expected that such mixtures would contain a large variety of compounds of different amine types, amino compound sizes, and ion structures.

18C6 Complexation and IMS-IMS-MS Measurements for VGO Distillate Characterization

A series of preliminary studies of the VGO distillate sample were performed to optimize these experiments. Multiple

relative reagent concentrations (VGO:18C6=20:1, 10:1, 5:1, 2:1, 1:1, 1:2, 1:5, and 1:10, and concentration ranges for VGO between 1 and 5 mg mL^{-1}) were tested in order to obtain the best solution conditions for the petroleomics analysis. Maximum complexation is achieved when the concentration for the VGO distillate is ~2 to 3 mg mL^{-1} and the VGO:18C6 ratio is 1:2. As before, only the mobility ranges for $[M + 18C6 + H]^+$ ion complexes were selected for analysis to improve dataset interpretability.

Figure 5 shows typical results obtained upon electrospraying the VGO distillate sample without 18C6 (Figure 5a), with the addition of 18C6 (Figure 5b) and with the addition of 18C6 employing IMS-IMS separations (Figure 5c, 80 V activation voltage). Figure 5a shows that the $[M + H]^+$ ions in the VGO distillate sample have a *m/z* distribution ranging from ~170 to ~330 and a drift time distribution ranging from ~10 ms to ~17 ms. Also shown in Figure 5a, is a series of $[M_1 + M_2 + H]^+$ dimer ions ranging from *m/z* ~450 to ~600 and having a drift time range of ~18 to ~24 ms.

When 18C6 is added to the VGO distillate sample solution, 18C6 forms complexes with amino compounds in the VGO distillate sample. Here we note that in the complex VGO distillate sample other molecules may exist that form complexes with 18C6. Previous work performed using a similar VGO distillate sample has shown that the dominant features in ESI mass spectra of basic compounds are comprised of ~75% amine containing molecules [80]. The remainder of the dominant features is primarily oxygen/sulfur species. Because of this prevalence of amino compounds as well as the fact that the dominant features observed and compared in these datasets

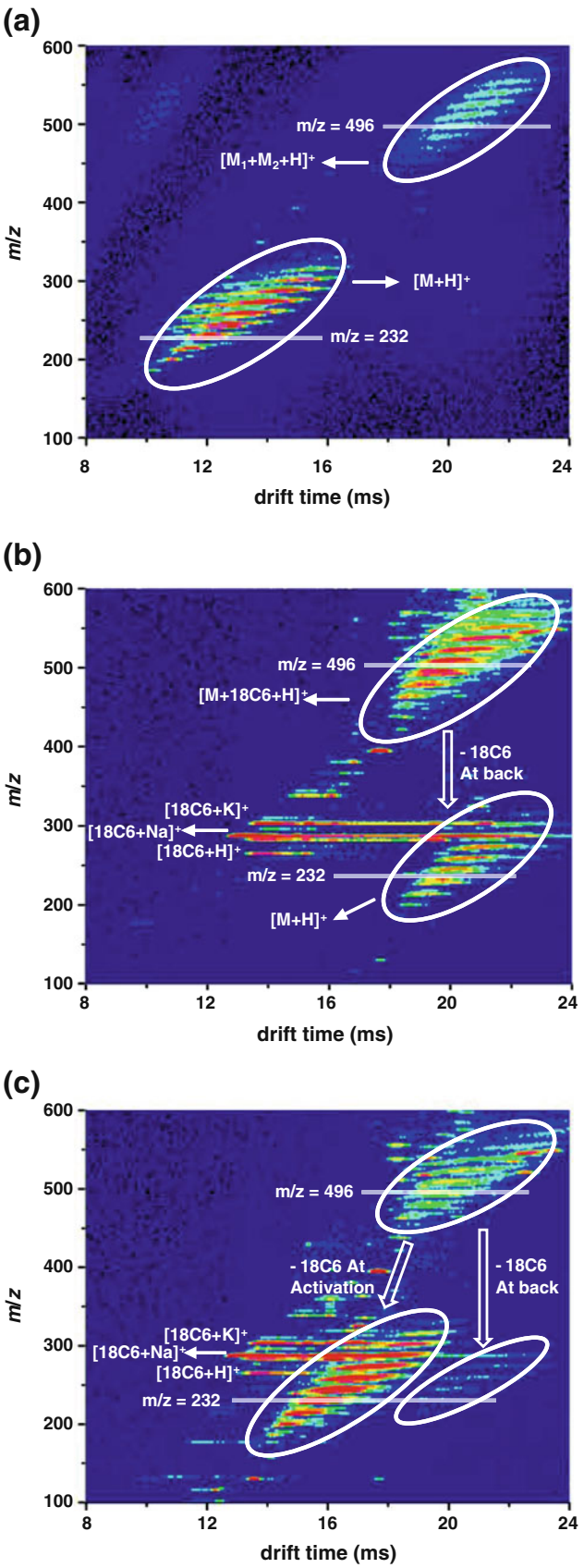

Figure 5. Two dimensional dot plots of drift time versus *m/z* ▶ obtained from ESI-IMS-MS experiments for a low-boiling VGO distillate sample. Panel (**a**) shows data collected for a VGO distillate sample without activation where the $[M + H]^+$ and $[M_1 + M_2 + H]^+$ ion regions are shown with white ovals. Regions selected for IMS distribution comparisons (Figure 6) are shown as solid lines at *m/z*=232 and *m/z* 496. Panel (**b**) shows data collected for the VGO distillate sample upon addition of 18C6. Here no activation voltage is employed. White ovals indicate the $[M + 18C6 + H]^+$ ion region and the region occupied by the $[M + H]^+$ ions generated by dissociation of 18C6-ion complexes at the end of F3. Solid lines at *m/z*=232 and *m/z* 496 indicate regions used for drift time distribution comparisons (Figure 6). Prominent 18C6 ions are labeled. Panel (**c**) shows data collected for the VGO distillate sample with 18C6 where 80 V activation has been employed in the IA2 region (Figure 1). White ovals indicate the $[M + 18C6 + H]^+$ ion region and the region occupied by the $[M + H]^+$ ions generated by dissociation of 18C6-ion complexes in the IA2 region as well as those formed at the end of F3. Solid lines at *m/z*=232 and *m/z* 496 indicate regions used for drift time distribution comparisons (Figure 6). Prominent 18C6 ions are labeled. The intensities of different features in all dot plots are represented here using a false color scheme in which the least intense features are shown in dark blue and the most intense are shown in red

contain even *m/z* values, ions are referred to as 18C6–amino compound complexes. IMS-MS experiments (Figure 5b) of the VGO distillate sample with 18C6 indicate the presence of $[M + 18C6 + H]^+$ ion complexes, having a *m/z* distribution ranging from ~430 to ~600 and a drift time distribution ranging from ~17 ms to ~24 ms. At lower *m/z* values, a number of features are observed over the same drift time range corresponding to $[M + H]^+$ ions arising from dissociation of $[M + 18C6 + H]^+$ ion complexes at the end of F3 (Figure 5b). High-intensity 18C6 ions, such as $[18C6 + H]^+$, $[18C6 + Na]^+$,and $[18C6 + K]^+$ are also observed.

When an activation step is utilized between the two IMS steps, a portion of the $[M + 18C6 + H]^+$ ion complexes dissociates into $[M + H]^+$ ions and 18C6 molecules. The smaller $[M + H]^+$ ions have larger mobilities than their $[M + 18C6 + H]^+$ ion precursors, and differ in *m/z* values by 264.157 Da (a single 18C6 molecule). The percentage of dissociated $[M + 18C6 + H]^+$ ion precursors increases as the activation voltage is raised from 40 V to 60, 80, and 100 V. Figure 5b shows that many of the $[M + 18C6 + H]^+$ ion complexes do not dissociate at the 40 V activation voltage settings. However, Figure 5c shows that when 80 V activation voltage is used, the majority of the $[M + 18C6 + H]^+$ ion complexes dissociate to form $[M + H]^+$ ions as demonstrated by the features observed over the drift time range of ~14 to ~20 ms having a *m/z* range of ~175 to ~325. In addition, a small amount of the $[M + 18C6 + H]^+$ ion complexes is observed to fragment at the end of F3.

In order to observe the separation achieved with the addition of 18C6 and the incorporation of an ion activation step in more detail, drift time distributions were extracted at nominal masses of *m/z*=232 (Figure 6a) and *m/z*=496 (Figure 6b). Drift time distributions obtained from six

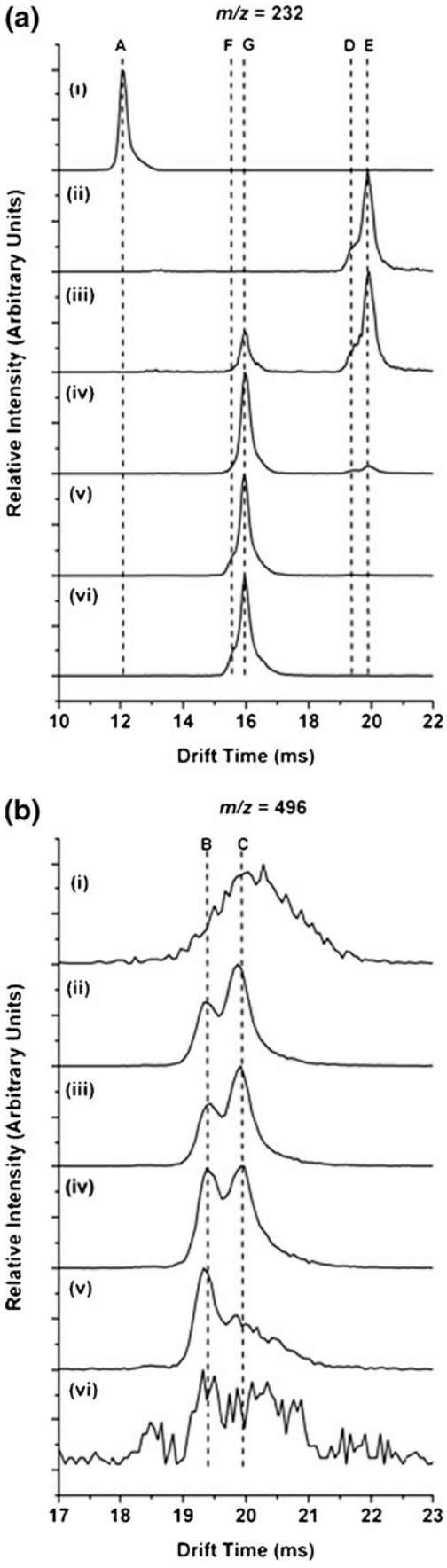

Figure 6. Drift time distributions obtained for experiments for the VGO distillate samples with and without 18C6. Data are represented for different experimental conditions (with varying amounts of ion activation in the IA2 region as well as no activation). Panels (**a**) and (**b**) show distributions at *m/z*= 232 and 496, respectively, for the VGO distillate sample. Part (i) in both panels shows data obtained in the absence of 18C6 and without the use of ion activation at IA2. Part (ii) in both panels shows data obtained in the presence of 18C6. Again, no activation voltage is employed. Parts (iii), (iv), (v), and (vi) show drift time distributions for the VGO distillate sample with 18C6 using activation voltages of 40, 60, 80, and 100 V activation in the IA2 region. Feature A indicates the peak position (~12.1 ms) in the drift time distribution of the $[M + H]^+$ ions with nominal *m/z*=232. Features B and C correspond to the peak positions of $[M + 18C6 + H]^+$ ions with nominal *m/z*=496 at ~19.3 ms and ~19.9 ms, respectively. Features D and E represent the $[M + H]^+$ ions at nominal *m/z*=232, which are formed from dissociation of $[M + 18C6 + H]^+$ ions (Features B and C, respectively) at the end of F3 prior to TOF analysis. Features F and G mark the peak positions at ~15.8 and ~16.0 ms of the $[M + H]^+$ ions at nominal *m/z*=232, which are formed at IA2 from dissociation of $[M + 18C6 + H]^+$ ions from (Features B and C)

datasets are given as examples in Figure 6 including: (i) the VGO distillate sample without 18C6 from an IMS-MS experiment; (ii) the VGO distillate sample with 18C6 from an IMS-MS experiment; (iii) the VGO distillate sample with 18C6 from an IMS-IMS-MS experiment employing 40 V activation voltage in IA2; and the same sample with (iv) 60 V activation voltage; (v) 80 V activation voltage, and (vi) 100 V activation voltage.

The extracted drift time distributions shown in Figure 6a(i) reveal that the $[M + H]^+$ ions having m/z= 232 appear to comprise a single peak (Feature A) at ~12.1 ms. The full width at half maximum (FWHM) for feature **A** is ~0.29 ms. Applying a Gaussian fit ($\bar{x} = 12.101$, σ=0.129, R^2=0.969) to the experimental data provides a FWHM of ~0.30 ms. The resolving power calculated for this peak (~40) is lower than the typical resolving power of this 2 m drift tube (~70 to 80) by a factor of ~2 suggesting the presence of isobaric ions and/or multiple gas-phase conformations. That said, the relatively narrow peak corresponding to **A** indicates that the multiple mixture components in this m/z region have very similar mobilities. The drift time distribution of the $[M_1 + M_2 + H]^+$ dimer ions [Figure 6b(i)] at m/z=496 shows a broad feature existing over a drift time range of ~18.5 ms to ~21.5 ms indicating a broader range of different ion sizes for these species.

When 18C6 is added to the VGO distillate sample, the $[M + 18C6 + H]^+$ ion complexes formed with m/z 496 separate into two features as shown in Figure 6b(ii). These include features **B** and **C** at ~19.3 ms and ~19.9 ms, respectively. The FWHM for either feature is difficult to measure; however, a Gaussian fit ($\bar{x} = 19.341$, σ=0.138; and $\bar{x} = 19.874$, σ=0.217, respectively) provides FWHMs for **B** and **C** of ~0.33 ms and ~0.51 ms, respectively. The peak height ratio for the peaks obtained from the fit is 1:1.62 (**B**:**C**). The existence of the two features (Features B and C in Figure 6b) in the drift time distribution for the $[M + 18C6 + H]^+$ ion complexes compared with the constituent $[M + H]^+$ ions (Feature A in Figure 6a) suggests that the incorporation of 18C6 may provide a means for increasing the separation capacity compared with IMS measurements of the protonated species. This is consistent with the improved separation of the model compounds NOA and DBA obtained by adding 18C6 to the amine mixture (Figure 2). Similarly, **B** and **C** (Figure 6) may represent separate classes of amino compounds in this complex mixture.

At the end of F3, some of the $[M + 18C6 + H]^+$ ion complexes dissociate into $[M + H]^+$ ions as depicted in Figure 6a(ii). These ions (features **D** and **E** in Figure 6a) represent the nitrogen-containing compounds that comprise the $[M + 18C6 + H]^+$ ion complexes depicted by **B** and **C** [Figure 6b(ii)]. It is noted that many more monomer ions appear to result from dissociation of **C** compared with those arising from **B**. This difference reflects the relative stabilities of the $[M + 18C6 + H]^+$ ion complexes comprising **B** and **C** providing further evidence of a separation of molecular classes with different structures.

To explore how the differences in gas phase stabilities may be utilized to enhance the separation of petroleomics mixture components, IMS-IMS-MS experiments were performed at a variety of activation voltages. As shown in Figure 6b, the relative intensity for **C** decreases more rapidly than that for **B,** such that at 60 V activation voltage [Figure 6b(iv)] the two peaks have the same intensity. **B** becomes the dominant peak at 80 V activation voltage [Figure 6b(v)]. The peak height ratios (B:C) provided by Gaussian fits at 40, 60, and 80 V activation voltages are 1:1.58, 1:1.10, and 1:0.58, respectively. Noticeably, at 80 V, **C** merges into the tail of **B** forming a broad tail. This suggests that ions with many different structures may comprise **C**. At 100 V activation voltage [Figure 6b(vi)], the majority of complexes comprising **B** and **C** dissociate. The $[M + 18C6 + H]^+$ ion complexes that dissociate form $[M + H]^+$ ions with m/z values of 232. Because dissociation occurs between drift separation steps, the fragment ions have shorter drift times than the precursor complex ions. Fragment ions produced by dissociation of **B** and **C** in the IA2 region are shown as features **F** and **G** in Figure 6a. Because **G** arises from dissociation of the less stable complexes represented by **C**, it is observed at a lower activation voltage. **F** is only observed as a shoulder on **G** after 80 V activation voltage is employed. The two features are not as highly resolved as the $[M + 18C6 + H]^+$ ion complexes because they are only separated as the complexes in the first drift stage (D1). During the second drift separation step (D2), these ions exhibit similar mobilities [Figure 6a(i)].

Summary and Conclusions

The complexation of 18C6 to amino compounds has been examined as a means for characterization of mixtures of these species by multidimensional IMS-MS techniques. The data show that the addition of excess 18C6 to mixtures of model amino compounds enhances component resolution, which arises from differences in the physical size of the complexes formed. Additionally, increased selectivity is achieved based on the stabilities of $[M + 18C6 + H]^+$ ion complexes; in general, ion complex stabilities are observed to be inversely correlated to amino compound GB. Factors affecting ion complex stabilities include the structure of the amine group as well as the structure and size of the amino compound ion. The application of 18C6 complexation with IMS-IMS analysis of a petroleomics sample demonstrates improved resolution of select, nitrogen-containing compounds. IMS-IMS techniques are interesting as a means of separation because they provide enhancements in separation that are gained from both the changes in physical size of the complexes as well as the differences in the stabilities of the complexes.

Acknowledgments

The authors gratefully acknowledge finnancial support from grants provided by the National Institutes of Health (NIA R01 AG024547), the Next Generation Threat Fund from Naval Surface Warfare Center-Crane Division (contract number N00164-08-C-JQ11), and the Knowledge Build Fund from ExxonMobil (ExxonMobil Research and Engineering Company, Annandale, NJ). The authors are grateful for enlightening discussions with Dr. Kuangnan Qian from ExxonMobile as well as for providing the VGO distillate sample.

References

1. Mason, E.A., McDaniel, E.W.: Transport Properties of Ions in Gases. Wiley, New York (1988)
2. St Louis, R.H., Hill, H.H.: Ion mobility spectrometry in analytical chemistry. *CRC Crit. Rev. Anal. Chem* **21**, 321–355 (1990)
3. Eiceman, G.A., Rodriguez, J.E., Parmeter, J.E. Trace Detection of Narcotics Using a Preconcentrator/Ion Mobility Spectrometer System; NIJ Report 602-00; National Institute of Justice: Washington, DC, April, (2001).
4. Eiceman, G.A., Karpas, Z.: Ion Mobility Spectrometry, 2nd edn, p. 360. CRC, Boca Raton (2005)
5. Dubnikova, F., Kosloff, R., Zeiri, Y., Karpas, Z.: Novel approach to the detection of triacetone triperoxide (TATP): Its structure and its complexes with ions. *J. Phys. Chem. A* **106**(19), 4951–4956 (2002)
6. Hill Jr., H.H., Martin, S.J.: Conventional analytical methods for chemical warfare agents. *Pure Appl. Chem.* **74**(12), 2281–2291 (2002)
7. Creaser, C.S., Griffiths, J.R., Bramwell, C.J., Noreen, S., Hill, C.A., Thomas, C.L.P.: Ion mobility spectrometry: A review. Part 1. Structural analysis by mobility measurement. *Analyst* **129**(11), 984–994 (2004)
8. Hill Jr., H.H., Steiner, W.E.: Ion mobility spectrometry for monitoring the destruction of chemical warfare agents. In: Kolodkin, V.M., Ruck, W. (eds.) Ecological Risks Associated with the Destruction of Chemical Weapons, pp. 157–166. Springer Netherlands, Luneburg (2006)
9. Hoaglund, C.S., Valentine, S.J., Sporleder, C.R., Reilly, J.P., Clemmer, D.E.: Three-dimensional ion mobility/TOFMS analysis of electrosprayed biomolecules. *Anal. Chem.* **70**(11), 2236–2242 (1998)
10. Henderson, S.C., Valentine, S.J., Counterman, A.E., Clemmer, D.E.: ESI/ion trap/ion mobility/time-of-flight mass spectrometry for rapid and sensitive analysis of biomolecular mixtures. *Anal. Chem.* **71**(2), 291–301 (1999)
11. Hoaglund-Hyzer, C.S., Counterman, A.E., Clemmer, D.E.: Anhydrous protein ions. *Chem. Rev.* **99**(10), 3037–3079 (1999)
12. Srebalus, C.A., Li, J., Marshall, W.S., Clemmer, D.E.: Gas-phase separations of electrosprayed peptide libraries. *Anal. Chem.* **71**(18), 3918–3927 (1999)
13. Hoaglund-Hyzer, C.S., Clemmer, D.E.: Ion trap/ion mobility/quadrupole/time-of-flight mass spectrometry for peptide mixture analysis. *Anal. Chem.* **73**(2), 177–184 (2001)
14. Jarrold, M.F.: Peptides and proteins in the vapor phase. *Annu. Rev. Phys. Chem.* **51**, 179–207 (2000)
15. Liu, X., Valentine, S.J., Plasencia, M.D., Trimpin, S., Naylor, S., Clemmer, D.E.: Mapping the human plasma proteome by SCX-LC-IMS-MS. *J. Am. Soc. Mass Spectrom.* **18**(7), 1249–1264 (2007)
16. Trimpin, S., Plasencia, M., Isailovic, D., Clemmer, D.E.: Resolving oligomers from fully grown polymers with IMS-MS. *Anal. Chem.* **79** (21), 7965–7974 (2007)
17. Bohrer, B.C., Merenbloom, S.I., Koeniger, S.L., Hilderbrand, A.E., Clemmer, D.E.: Biomolecule analysis by ion mobility spectrometry. *Annu. Rev. Anal. Chem.* **1**, 293–327 (2008)
18. Plasencia, M.D., Isailovic, D., Merenbloom, S.I., Mechref, Y., Clemmer, D.E.: Resolving and assigning N-linked glycan structural isomers from ovalbumin by IMS-MS. *J. Am. Soc. Mass Spectrom.* **19** (11), 1706–1715 (2008)
19. Von Helden, G., Hsu, M.T., Kemper, P.R., Bowers, M.T.: Structures of carbon cluster ions from 3 to 60 atoms: Linears to rings to fullerenes. *J. Chem. Phys.* **95**(5), 3835–3837 (1991)
20. Jarrold, M.F., Constant, V.A.: Silicon cluster ions: Evidence for a structural transition. *Phys. Rev. Lett.* **67**, 2994–2997 (1991)
21. Bowers, M.T., Kemper, P.R., Von Helden, G., Van Koppen, P.A.M.: Gas-phase ion chromatography: Transition metal state selection and carbon cluster formation. *Science* **260**, 1446–1451 (1993)
22. Hunter, J., Fye, J., Jarrold, M.F.: Annealing $C60^+$: Synthesis of fullerenes and large carbon rings. *Science* **260**, 784–786 (1993)
23. Clemmer, D.E., Hudgins, R.R., Jarrold, M.F.: Naked protein conformations: Cytochrome *c* in the gas phase. *J. Am. Chem. Soc.* **117**, 10141–10142 (1995)
24. Valentine, S.J., Anderson, J.G., Ellington, A.D., Clemmer, D.E.: Disulfide-intact and -reduced lysozyme in the gas phase: Conformations and pathways of folding and unfolding. *J. Phys. Chem. B* **101**, 3891–3900 (1997)
25. Wu, C., Siems, W.F., Klasmeier, J., Hill, H.H.: Separation of isomeric peptides using electrospray ionization/high-resolution ion mobility spectrometry. *Anal. Chem.* **72**(2), 391–395 (2000)
26. Creaser, C.S., Benyezzar, M., Griffiths, J.R., Stygall, J.W.: A tandem ion trap/ion mobility spectrometer. *Anal. Chem.* **72**(13), 2724–2729 (2000)
27. Hill, H.H., Hill, C.H., Asbury, G.R., Wu, C., Matz, L.M., Ichiye, T.: Charge location on gas phase peptides. *Int. J. Mass Spectrom.* **219**, 23–37 (2002)
28. Srebalus, C.A., Li, J.W., Marshall, W.S., Clemmer, D.E.: Determining synthetic failures in combinatorial libraries by hybrid gas-phase separation methods. *J. Am. Soc. Mass Spectrom.* **11**(4), 352–355 (2000)
29. Dugourd, P.H., Hudgins, R.R., Clemmer, D.E., Jarrold, M.F.: High-resolution ion mobility measurements. *Rev. Sci. Instrum.* **68**, 1122–1129 (1997)
30. Wu, C., Siems, W.F., Asbury, G.R., Hill, H.H.: Electrospray ionization high-resolution ion mobility spectrometry-mass spectrometry. *Anal. Chem.* **70**(23), 4929–4938 (1998)
31. Asbury, G.R., Hill, H.H.: Evaluation of ultrahigh resolution ion mobility spectrometry as an analytical separation device in chromatographic terms. *J. Microcolumn Sep.* **12**, 172–178 (2000)
32. Tang, K., Shvartsburg, A.A., Lee, H., Prior, D.C., Buschbach, M.A., Li, F., Tomachev, A., Anderson, G.A., Smith, R.D.: High-sensitivity ion mobility spectrometry/mass spectrometry using electrodynamic ion funnel interfaces. *Anal. Chem.* **77**(10), 3330–3339 (2005)
33. Koeniger, S.L., Merenbloom, S.I., Valentine, S.J., Udseth, H., Smith, R. D., Clemmer, D.E.: An IMS-IMS analogue of MS-MS. *Anal. Chem.* **78** (12), 4161–4174 (2006)
34. Merenbloom, S.I., Koeniger, S.L., Valentine, S.J., Plasencia, M.D., Clemmer, D.E.: IMS-IMS and IMS-IMS-IMS/MS for separating peptide and protein fragment ions. *Anal. Chem.* **78**(8), 2802–2809 (2006)
35. Gillig, K.J., Ruotolo, B.T., Stone, E.G., Russell, D.H.: An electrostatic focusing ion guide for ion mobility-mass spectrometry. *Int. J. Mass Spectrom.* **239**, 43–49 (2004)
36. Kemper, P.R., Dupuis, N.F., Bowers, M.T.: A new, higher resolution, ion mobility mass spectrometer. *Int. J. Mass Spectrom.* **287**, 46–57 (2009)
37. Merenbloom, S.I., Glaskin, R.S., Henson, Z.B., Clemmer, D.E.: High-resolution ion cyclotron mobility spectrometry. *Anal. Chem.* **81**(4), 1482–1487 (2009)
38. Glaskin, R.S., Valentine, S.J., Clemmer, D.E.: A scanning frequency mode for ion cyclotron mobility spectrometry. *Anal. Chem.* **82**(19), 8266–8271 (2010)
39. Shvartsburg, A.A., Danielson, W.F., Smith, R.D.: *Anal. Chem.* **82**(6), 2456–2462 (2010)
40. Shvartsburg, A.A., Prior, D.C., Tang, K.Q., Smith, R.D.: High-resolution differential ion mobility separations using planar analyzers at elevated dispersion fields. *Anal. Chem.* **82**(18), 7649–7655 (2010)
41. Tang, K.Q., Li, F.M., Shvartsburg, A.A., Strittmatter, E.F., Smith, R.D.: Two-dimensional gas-phase separations coupled to mass spectrometry for analysis of complex mixtures. *Anal. Chem.* **77**(19), 6381–6388 (2005)
42. Merenbloom, S.I., Bohrer, B.C., Koeniger, S.L., Clemmer, D.E.: Assessing the peak capacity of IMS-IMS separations of tryptic peptide ions in He at 300 K. *Anal. Chem.* **79**(2), 515–522 (2007)
43. Kurulugama, R.T., Valentine, S.J., Sowell, R.A., Clemmer, D.E.: Development of a high-throughput IMS-IMS-MS approach for analyzing mixtures of biomolecules. *J. Proteomics* **71**(3), 318–331 (2008)
44. Merenbloom, S.I., Koeniger, S.L., Bohrer, B.C., Valentine, S.J., Clemmer, D.E.: Improving the efficiency of IMS-IMS by a combing technique. *Anal. Chem.* **80**(6), 1918–1927 (2008)

45. Polfer, N.C., Bohrer, B.C., Plasencia, M.D., Paizs, B., Clemmer, D. E.: On the dynamics of fragment isomerization in collision-induced dissociation of peptides. *J. Phys. Chem. A* **112**(6), 1286–1293 (2008)
46. Trimpin, S., Clemmer, D.E.: Ion mobility spectrometry/mass spectrometry snapshots for assessing the molecular compositions of complex polymeric systems. *Anal. Chem.* **80**(23), 9073–9083 (2008)
47. Valentine, S.J., Kurulugama, R.T., Bohrer, B.C., Merenbloom, S.I., Sowell, R.A., Mechref, Y., Clemmer, D.E.: Developing IMS-IMS-MS for rapid characterization of abundant proteins in human plasma. *Int. J. Mass Spectrom.* **283**(1/3), 149–160 (2009)
48. Lee, Y.J., Hoaglund-Hyzer, C.S., Taraszka, J.A., Zientara, G.A., Counterman, A.E., Clemmer, D.E.: Collision-induced dissociation of mobility-separated ions using an orifice-skimmer cone at the back of a drift tube. *Anal. Chem.* **73**(15), 3549–3555 (2001)
49. Belov, M.E., Clowers, B.H., Prior, D.C., Danielson, W.F., Liyu, A.V., Petritis, B.O., Smith, R.D.: Dynamically multiplexed ion mobility time-of-flight mass spectrometry. *Anal. Chem.* **80**(15), 5873–5883 (2008)
50. Clowers, B.H., Siems, W.F., Hill, H.H., Massick, S.M.: Hadamard transform ion mobility spectrometry. *Anal. Chem.* **78**(1), 44–51 (2006)
51. Williamson, B.L., Creaser, C.S.: Noncovalent inclusion complexes of protonated amines with crown ethers. *Int. J. Mass Spectrom.* **188**(1/2), 53–61 (1999)
52. Creaser, C.S., Griffiths, J.R., Stockton, B.M.: Gas-phase ion mobility studies of amines and polyether/amine complexes using tandem quadrupole ion trap/ion mobility spectrometry. *Eur. J. Mass Spectrom.* **6**(2), 213–218 (2000)
53. Colgrave, M.L., Bramwell, C.J., Creaser, C.S.: Nanoelectrospray ion mobility spectrometry and ion trap mass spectrometry studies of the noncovalent complexes of amino acids and peptides with polyethers. *Int. J. Mass Spectrom.* **229**(3), 209–216 (2003)
54. Hilderbrand, A.E., Myung, S., Clemmer, D.E.: Exploring crown ethers as shift reagents for ion mobility spectrometry. *Anal. Chem.* **78**(19), 6792–6800 (2006)
55. Howdle, M.D., Eckers, C., Laures, A.M.F., Creaser, C.S.: The use of shift reagents in ion mobility-mass spectrometry: Studies on the complexation of an active pharmaceutical ingredient with polyethylene glycol excipients. *J. Am. Soc. Mass Spectrom.* **20**(1), 1–9 (2009)
56. Maleknia, S., Brodbelt, J.: Cavity-size-dependent dissociation of crown ether/ammonium ion complexes in the gas phase. *J. Am. Chem. Soc.* **115**(7), 2837–2843 (1993)
57. Liou, C.C., Wu, H.F., Brodbelt, J.S.: Hydrogen-bonding interactions in gas-phase polyether/ammonium ion complexes. *J. Am. Soc. Mass Spectrom.* **5**(4), 260–273 (1994)
58. Alvarez, E.J., Wu, H.-F., Liou, C.-C., Brodbelt, J.: Collisionally activated dissociation of transition metal ion/polyether complexes in a quadrupole ion trap. *J. Am. Chem. Soc.* **118**(38), 9131–9138 (1996)
59. Alvarez, E.J., Vartanian, V.H., Brodbelt, J.S.: Dissociation of polyether-transition metal ion dimer complexes in a quadrupole ion trap. *J. Am. Soc. Mass Spectrom.* **8**(6), 620–629 (1997)
60. David, W.M., Brodbelt, J.S.: Threshold dissociation energies of protonated amine/polyether complexes in a quadrupole ion trap. *J. Am. Soc. Mass Spectrom.* **14**(4), 383–392 (2003)
61. Crowe, M.C., Brodbelt, J.S.: Evaluation of noncovalent interactions between peptides and polyether compounds via energy-variable collisionally activated dissociation. *J. Am. Soc. Mass Spectrom.* **14**(10), 1148–1157 (2003)
62. Becker, C., Qian, K., Russell, D.H.: Molecular weight distributions of asphaltenes and deasphaltened oils studied by laser desorption ionization and ion mobility mass spectrometry. *Anal. Chem.* **80**(22), 8592–8597 (2008)
63. Fernandez-Lima, F.A., Becker, C., McKenna, A.M., Rodgers, R.P., Marshall, A.G., Russel, D.H.: Petroleum crude oil characterization by IMS-MS and FTICR MS. *Anal. Chem.* **81**(24), 9941–9947 (2009)
64. Marshall, A.G., Rodgers, R.P.: Petroleomics: The next grand challenge for chemical analysis. *Acc. Chem. Res.* **37**(1), 53–59 (2004)
65. Marshall, A.G., Rodgers, R.P.P.: Petroleomics: Chemistry of the underworld. *Proc. Natl. Acad. Sci. U. S. A.* **10**(47), 18090–18095 (2008)
66. Rodgers, R.P., Marshall, A.G.: Petroleomics: Advanced characterization of petroleum-derived materials by fourier transform ion cyclotron resonance mass spectrometry (FT-ICR MS). In: Mullins, O.C., Sheu, E.Y., Hammami, A., Marshall, A.G. (eds.) Asphaltenes, Heavy Oils, and Petroleomics, 1st edn, pp. 63–93. Springer, New York (2007)
67. Speight, J.G.: Handbook of Petroleum Analysis, pp. 25–59. Wiley-Interscience, New York (2001)
68. Mullins, O.C., Rodgers, R.P., Weinheber, P., Klein, G.C., Venkataramanan, L., Andrews, A.B., Marshall, A.G.: Oil reservoir characterization via crude oil analysis by downhole fluid analysis in oil wells with visible near-infrared spectroscopy and by laboratory analysis with electrospray ionization fourier transform ion cyclotron resonance mass spectrometry. *Energy Fuels* **20**(6), 2448–2456 (2006)
69. Betancourt, S.S., Ventura, G.T., Pomerantz, A.E., Viloria, O., Dubost, F.X., Zuo, J., Monson, G., Bustamante, D., Purcell, J.M., Nelson, R.K., Rodgers, R.P., Reddy, C.M., Marshall, A.G., Mullins, O.C.: Nanoaggregates of asphaltenes in a reservoir crude oil and reservoir connectivity. *Energy Fuels* **23**(3), 1178–1188 (2009)
70. Loeb, L.B.: Basic Processes of Gaseous Electronics, 2nd edn, p. 1028. California, Berkeley and Los Angeles (1955)
71. Liu, Y., Valentine, S.J., Counterman, A.E., Hoaglund, C.S., Clemmer, D.E.: Injected-ion mobility analysis of biomolecules. *Anal. Chem.* **69** (23), 728A–735A (1997)
72. Hoaglund-Hyzer, C.S., Li, J., Clemmer, D.E.: Mobility labeling for parallel CID of ion mixtures. *Anal. Chem.* **72**(13), 273–2740 (2000)
73. Valentine, S.J., Kulchania, M., Barnes, C.A.S., Clemmer, D.E.: Multidimensional separations of complex peptide mixtures: A combined high-performance liquid chromatography/ion mobility/time-of-flight mass spectrometry approach. *Int. J. Mass Spectrom.* **212**(1/3), 97–109 (2001)
74. Hoaglund-Hyzer, C.S., Lee, Y.J., Counterman, A.E., Clemmer, D.E.: Coupling ion mobility separations, collisional activation techniques, and multiple stages of MS for analysis of complex peptide mixtures. *Anal. Chem.* **74**(5), 992–1006 (2002)
75. Shaffer, S.A., Tolmachev, A., Prior, D.C., Anderson, G.A., Udseth, H. R., Smith, R.D.: Characterization of an improved electrodynamic ion funnel interface for electrospray ionization mass spectrometry. *Anal. Chem.* **71**(15), 2957–2964 (1999)
76. Shaffer, S.A., Tang, K.Q., Anderson, G.A., Prior, D.C., Udseth, H.R., Smith, R.D.: A Novel ion funnel for focusing ions at elevated pressure using electrospray ionization mass spectrometry. *Rapid Commun. Mass Spectrom.* **11**(16), 1813–1817 (1997)
77. Shaffer, S.A., Prior, D.C., Anderson, G.A., Udseth, H.R., Smith, R.D.: An ion funnel interface for improved ion focusing and sensitivity using electrospray ionization mass spectrometry. *Anal. Chem.* **70**(19), 4111–4119 (1998)
78. Meot-Ner, M.: The Ionic Hydrogen Bond. 3. Multiple Imidogen(1+)-Oxygen (NH+…O) and Methylidyne(.delta.+)-oxygen (CH.delta.+…O) Bonds. Complexes of ammonium ions with polyethers and crown ethers. *J. Am. Chem. Soc.* **105**(15), 4912–4915 (1983)
79. References are taken from the NIST database: http://webbook.nist.gov/
80. Stanford, L.A., Kim, S., Rodgers, R.P., Marshall, A.G.: Characterization of compositional changes in vacuum gas oil distillation cuts by electrospray ionization fourier transform-ion cyclotron resonance (FT-ICR) mass spectrometry. *Energy Fuels* **20**, 1664–1673 (2006)